Purinergic Signalling (2024) 20:273–284
https://doi.org/10.1007/s11302-023-09947-w

RESEARCH

Potential role of the P2X7 receptor in the proliferation of human diffused large B-cell lymphoma

Xiao Yang[1] · Yuanyuan Ji[1] · Lin Mei[1] · Wenwen Jing[1] · Xin Yang[2] · Qianwei Liu[3]

Received: 26 February 2023 / Accepted: 18 May 2023 / Published online: 24 May 2023

Abstract

Diffuse large B-cell lymphoma (DLBCL) is the most common subtype of invasive non-Hodgkin lymphoma. 60–70% of patients are curable with current chemoimmunotherapy, whereas the rest are refractory or relapsed. Understanding of the interaction between DLBCL cells and tumor microenvironment raises the hope of improving overall survival of DLBCL patients. P2X7, a member of purinergic receptors P2X family, is activated by extracellular ATP and subsequently promotes the progression of various malignancies. However, its role in DLBCL has not been elucidated. In this study, the expression level of *P2RX7* in DLBCL patients and cell lines was analyzed. MTS assay and EdU incorporation assay were carried out to study the effect of activated/inhibited P2X7 signaling on the proliferation of DLBCL cells. Bulk RNAseq was performed to explore potential mechanism. The results demonstrated high level expression of *P2RX7* in DLBCL patients, typically in patients with relapse DLBCL. 2′(3′)-O-(4-benzoylbenzoyl) adenosine 5-triphosphate (Bz-ATP), an agonist of P2X7, significantly accelerated the proliferation of DLBCL cells, whereas delayed proliferation was detected when administrated with antagonist A740003. Furthermore, a urea cycle enzyme named *CPS1* (carbamoyl phosphate synthase 1), which up-regulated in P2X7-activated DLBCL cells while down-regulated in P2X7-inhibited group, was demonstrated to involve in such process. Our study reveals the role of P2X7 in the proliferation of DLBCL cells and implies that P2X7 may serve as a potential molecular target for the treatment of DLBCL.

Keywords Diffuse large B-cell lymphoma · Purinergic receptor · P2X7 · Proliferation · CPS1

Introduction

DLBCL is the most common type of malignant lymphoid neoplasm in adults, comprising 30–40% of all new diagnosed non-Hodgkin lymphomas [1]. Although 60–70% of DLBCL patients are curable with first-line treatment R-CHOP (rituximab, cyclophosphamide, doxorubicin, vincristine and prednisolone), the rest respond poorly to standard therapy or will relapse with resistant disease [2]. The development of relapse and refractory DLBCL (rrDLBCL) consists of a complex series of events caused by aberrant cell signaling in both genetic and epigenetic abnormalities [3, 4]. Nucleotides have been suggested to be extracellular messengers for decades, and play important roles in promoting the process of malignant progression by activating purinergic receptors signaling [5]. The P2 purinergic receptors (P2Rs), which are activated by extracellular purine or pyrimidine nucleotides, can be divided into P2YR and P2XR family [6]. Most recently, P2YRs have been demonstrated to drive cancer cell growth by elevating intracellular Ca^{2+} and activating the PI3K-AKT and ERK-MAPK pathways [7]. P2XRs are demonstrated to directly or indirectly regulate tumor PI3K-GSK3β-dependent proliferation, VEGF-dependent angiogenesis, and dissemination [8–10]. However, the role of P2Rs in DLBCL development remains largely unknown. Elucidation of the molecular mechanisms underlying purinergic signaling in DLBCL progression, especially abnormal signaling transduction activated by extracellular

Xiao Yang and Yuanyuan Ji contributed equally to this work.

✉ Xiao Yang
yang_x@xjtu.edu.cn

[1] Scientific Research Center and Precision Medical Institute, The Second Affiliated Hospital, Xi'an Jiaotong University, Xi'an 710004, China

[2] Department of Rheumatology, The Second Affiliated Hospital, Xi'an Jiaotong University, Xi'an 710004, China

[3] Institute of Environmental Medicine, Karolinska Institutet, Stockholm 17177, Sweden

nucleotides, is important in the development of therapeutic strategies for patients with rrDLBCL.

P2X7, the latest cloned member of the P2X family receptors, differs in extra amino acids in the intracellular C terminus and is bi-functional [11]. The binding of ATP transiently induces the opening of a channel selective for small cations, whereas chronic ATP stimulation would lead to a non-selective pore opening, which allows permeation by molecules with a mass of up to 900 Da [12]. Previously, we demonstrated that P2X7 was preferentially expressed in more mature hematopoietic cells than hematopoietic stem and progenitor cells (HSPCs), and P2X7 can accelerate the progression of acute myeloid leukemia (AML) by promoting proliferation and increasing leukemia stem cells (LSCs) through the upregulation of Pre-B-Cell leukemia homeobox 3 (PBX3) [13, 14]. PBX3 has been reported to form specific and stable interactions with DNA in the absence of cofactors, and plays critical roles in the development and maintenance of a malignant phenotype [15]. In addition, abnormal up-regulated expression of P2X7 in patients with evolutive B-cell chronic lymphocytic leukemia (CLL) has been validated by other group few years ago [16]. Most importantly, a recent research reveals that ATP levels are markedly increased in the endosteal niche during leukemogenesis, and ATP-P2X7 signaling mediated cAMP response element-binding protein (CREB) / transactivated phosphoglycerate dehydrogenase (PHGDH) pathways are essential to maintain the homing and self-renewal capacities of leukemia initiating cells (LICs) [17]. Hence, abnormal expression and dysfunction of P2X7 plays important roles in different subtypes of leukemia.

Although abundant evidence suggests that the mediation role of P2X7 in purinergic signaling has been involved in leukemogenesis and progression, the effect of P2X7 signaling in DLBCL still remains largely unknown. In this study, we analyzed the expression level of *P2RX7* in DLBCL patients and cell lines, explored the effect of P2X7 in the proliferation of DLBCL cells, and performed bulk RNAseq to explain the molecular mechanism. Firstly, we confirmed that *P2RX7* expression was up-regulated in DLBCL samples and cell lines. Moreover, the activation of P2X7 signaling in DLBCL cell line OCI-Ly3 and SU-DHL-4 accelerated proliferation in vitro, while inhibition of P2X7 signaling significantly delayed cells proliferation. Additionally, carbamoyl phosphate synthase 1 (CPS1), a urea cycle enzyme, was essential for P2X7-mediate proliferation in DLBCL cells.

Materials and methods

Cell culture

The human ABC-DLBCL (activated B-cell-like diffuse large B-cell lymphoma) cell line OCI-Ly3 (RRID: CVCL_8800) is from DMSZ (Braunschweig, Germany), the human GCB-DLBCL (germinal center B-cell-like diffuse large B-cell lymphoma) cell line SU-DHL-4 (RRID: CVCL_0539) is from ATCC (Rockville, MD, USA), and the human CML (chronic myelogenous leukemia) cell line K562 (RRID: CVCL_0004) is from ATCC. Cells were maintained in RPMI-1640 Medium (Gibco, CA, USA) and supplemented with 10% FBS (Gibco, CA, USA), and kept in a humidified cell incubator (37 °C, 5% CO2, 95% humidity). Upon reaching semi-confluence, DLBCL cells were treated with the agonist 2′(3′)-O-(4-benzoylbenzoyl) adenosine 5-triphosphate (Bz-ATP) (Macklin, Shanghai, China) or the antagonist A740003 (Medchemexpress, NJ, USA) at different concentrations (0.05, 0.1, 0.5, 10, 20, 50, 100 μM) [18]. Treatments were carried out within 24 h, 48 or 72 h respectively for different experimental purpose.

GEPIA database analysis

GEPIA, a newly developed interactive web server for analyzing the RNA sequencing data of 9736 tumor samples and 8587 normal samples from the TCGA and GTEx projects [19]. In this study, GEPIA database was employed to analyze P2X receptor family members expression profiling in DLBCL patient samples (from TCGA data, n = 47) and normal control (from TCGA normal and GTEx data, n = 337). Briefly, input a gene symbol or id into the search box firstly, then find the bar plot of the gene expression profile across all tumor samples and paired normal tissues in the result, and recorded the expression value of target gene in DLBC group (short for diffused human diffused large B-cell lymphoma) respectively. Finally, we analyzed the expression value of P2X family genes in GraphPad. The expression level of genes was quantified by transcripts per million (TPM). TPM = (CDS read count × mean read length × 10^6) / (CDS length × total transcript count). TPM is a modification of RPKM designed to be consistent across samples, which normalized by total transcript count instead of read count in addition to average read length [20].

GEO dataset acquisition and analysis

The RNAseq or microarray datasets of DLBCL patients was downloaded from Gene Expression Omnibus (GEO) database (http://www.ncbi.nlm.nih.gov/geo/). Dataset GSE12195 contains 10 normal samples and 73 DLBCL

patient samples [21], GSE12453 contains 25 normal samples and 11 DLBCL patient samples [22], GSE25639 contains 13 normal samples and 26 DLBCL patient samples [23], and GSE32018 contains 6 samples and 22 DLBCL patient samples [24], all datasets were downloaded to analyze the expression level of *P2RX7* between normal and DLBCL patient. Dataset GSE65720 contains 20 DLBCL patient samples without relapse, 20 DLBCL samples from primary site and 20 DLBCL samples from relapsing site, which was downloaded to compare the different P2X7 DNA copy numbers [25]. Dataset GSE57611 contains 19 ABC-DLBCL samples and 18 GCB-DLBCL samples [26], GSE56315 contains 23 ABC-DLBCL samples and 29 GCB-DLBCL samples [27], GSE74266 contains 20 ABC-DLBCL samples and 22 GCB-DLBCL samples [28], and GSE32918 contains 80 ABC-DLBCL samples and 120 GCB-DLBCL samples [29], were downloaded to evaluate the expression level of *P2RX7* between ABC-DLBCL and GCB-DLBCL patients. Dataset GSE94669 contains 7 ABC-DLBCL cell lines samples and 20 GCB-DLBCL cell lines samples [30], GSE27255 contains 2 ABC-DLBCL cell lines samples and 12 GCB-DLBCL cell lines samples [31], all datasets were downloaded to determine the expression level of *P2RX7* in DLBCL cell lines, including both ABC and GCB subtype. Moreover, dataset GSE12195 was further analyzed to assess the expression relationships between *P2RX7* and *CPS1* in DLBCL patients [21].

cDNA synthesis and real time PCR

Cells were lysed with RNAex Pro reagent (AGbio, Hunan, China), and total RNA was isolated following the protocol of manufacture. Reverse transcription was achieved using PrimeScript™ 1st Strand Synthesis System (TAKARA, Tokyo, Japan). Realtime PCR was performed on the StepOne real-time PCR system (Applied Biosystems, CA, USA). The ΔΔCt method [$^{\Delta\Delta}Ct = (Ct_{TARGET} - Ct_{GAPDH})_{sample} - (Ct_{TARGET} - Ct_{GAPDH})_{calibrator}$] was used to analyze the gene expression level of target genes. The sequences for all primers were listed in Table 1.

Measurement of intracellular free Ca^{2+}

The intracellular free Ca^{2+} concentration was determined using the fluorescent indicator fura-2AM (Medchemexpress, NJ, USA). Briefly, DLBCL cells were incubated with 10 μM fura-2 at 37 °C for 20 min before being washed twice with Locke's solution (Pricella, Hubei, China) and then DLBCL cells were resuspended in Locke's solution at the concentration of $1X10^6$ cells/ml. The cell suspension was placed in 96-well plate and treated with 20 μM A740003 or Locke's solution for 5 min respectively. Then the fluorescence intensities at 510 nm excited separately by 340 and 380 nm laser were recorded every 12 s by SpectraMax iD5 (Molecular Devices, CA, USA). 50 μM Bz-ATP was added at indicated time point. The level of intracellular free Ca^{2+} was evaluated as fluorescence intensities at 510 nm which excited at 340 nm / fluorescence intensities at 510 nm which excited at 380 nm.

Cell proliferation assay

MTS assay (Promega, WI, USA) was used for cell proliferation analysis. OCI-Ly3 and SU-DHL-4 cells were seeded

Table 1 Primers used in this study

Gene	Sequence
P2RX7 (purinergic receptor P2X 7)	Forward 5'- CGACTAGGAGACATCTTCCGAG – 3' Reverse 5'- GCAGTGATGGAACCAACGGTCT – 3'
TLCD1 (TLC domain containing 1)	Forward 5'- CTTCGCTCACTCCATTGTGTCG – 3' Reverse 5'- AAAGTGACCACGCCGTCTCAATC – 3'
ABCA7 (ATP binding cassette subfamily A member 7)	Forward 5'- CACTCTTCCGAGAGCTAGACAC – 3' Reverse 5'- AAAGTGACCACGCCGTCTCAATC – 3'
ICAM5 (intercellular adhesion molecule 5)	Forward 5'- TCTCAGGCACTTACCGCTGCAA – 3' Reverse 5'- CTTCTGTTCCCTCCAGCCAAGT – 3'
RN7SL1 (RNA component of signal recognition particle 7SL1)	Forward 5'- GCTACTCGGGAGGCTGAGGCT – 3' Reverse 5'- TATTCACAGGCGCGATCC – 3'
SLX1B (SLX1 homolog B, structure-specific endonuclease subunit)	Forward 5'- CTGTGCCAGATGGACACTGAGA – 3' Reverse 5'- GTGGCACAGAAAAGAGGTAGGAG – 3'
DHRS2 (dehydrogenase/reductase 2)	Forward 5'- GGTGCTGTCATCCTGGTCTCTT – 3' Reverse 5'- CCAGCTCCAATGCCAGTGTTCT – 3'
CPS1 (carbamoyl-phosphate synthase 1)	Forward 5'- ATTCCTTGGTGTGGCTGAAC – 3' Reverse 5'- ATGGAAGAGAGGCTGGGATT – 3'
GAPDH (glyceraldehyde-3-phosphate dehydrogenase)	Forward 5'- GAAGGTGAAGGTCGGAGTC-3' Reverse 5'- GAAGATGGTGATGGGATTTC-3'

into 96-well plates at the concentration of $5X10^3$ cells/well and cultured for 4 h (designated as starting point, or 0 h point). Then cells were treated with PBS, 50 μM Bz-ATP, 50 μM A740003 respectively or treated with both 50 μM Bz-ATP and 20 μM A740003, cultured for extended periods. MTS (20 μl/well) was added to culture systems 2 h prior to evaluate the optical density (OD) at 490 nm every 24 h by SpectraMax iD5.

EdU incorporation assay

The EdU incorporation assay was performed by Beyo-Click™ EdU Cell Proliferation Kit with Alexa Fluor 488 (Beyotime, Shanghai, China) following the protocol of manufactures. Briefly, after Bz-ATP or A740003 administration, the OCI-Ly3 and SU-DHL-4 cells were incubated with 50 μM EdU for 2 h. After fixation and permeabilization, the incorporated EdU was visualized by means of a click reaction using Alexa Fluor 488 azide (30 min, room temperature). The nuclear DNA was stained by DAPI (10 μM, 30 min, room temperature). The images were obtained by a fluorescent microscope Axio Observer3 (Zeiss, Oberkochen, Germany). The Alexa Fluor 488 positive cells were adjusted to pseudo red color. The data were analyzed using ImageJ (NIH) software 1.52a and the proliferation rate was quantified as percentage of EdU^+ cell count / $DAPI^+$ cell count.

RNA sequencing and data analysis

SU-DHL-4 cells were treated with PBS, 50 μM Bz-ATP or 50 μM A740003 for 48 h respectively and then collected. RNA-seq was carried out by Benagen (Hubei, China) following standard protocols. The library products were sequenced using an Illumina NovaSeq platform. Standard bioinformatics analysis was performed by Benagen. The RNA-seq data of DLBCL-control, DLBCL-Bz-ATP and DLBCL-A740003 were available in the National Center for Biotechnology Information Gene Expression Omnibus database under accession number GSE225174. Different expression genes (DEGs) were filtrated by fold change (FC) > 2 and false discovery rate (FDR) < 0.05. The expression pattern was analyzed by K-Mean Cluster method using MultiExperimentViewer (MeV 4.9.0) software. The KEGG pathway were analyzed by OmicShare tools, an online platform for data analysis (https://www.omicshare.com/tools). The KEGG pathways were mainly filtrated by q value. The KEGG pathways with top 20 minimum q value were shown.

Ammonia assay

The ammonia levels in the conditioned media were measured using an ammonia assay kit (Abcam, Cambridge, MA) according to the instruction of manufacturers. Briefly, a total of $2X10^5$ SU-DHL-4 cells/well were plated into 12-well plates in antibiotic-free complete medium overnight, incubated with A740003 in conditioned media for 48 h, then medium was collected and centrifuged at 500 × g at 4 °C for 5 min to remove debris. Then the supernatant was transferred to a clean tube and kept on ice. 50 μl of each sample supernatant was diluted with 100 μl assay buffer, then added 50 μl of reaction mix solution into each sample well (50 μl sample dilution / well), mix and incubate at 37 °C for 60 min protected from light. The OD 570 nm was evaluated immediately by SpectraMax iD5 and normalized by cell number.

Statistical analysis

Data are presented as the mean ± SD. Differences between two groups were compared using a two-tailed unpaired Student's t-tests. Statistical analyses were performed using GraphPad 7 (San Diego, CA, USA). Statistical significance was accepted when the P values were less than 0.05.

Results

P2X7 is highly expressed in DLBCL patients and cell lines

The expression level of P2X family receptors was firstly evaluated by the GEPIA online tool (http://gepia.cancer-pku.cn/) [19]. Compared with adjacent normal tissues, *P2RX4*, *P2RX5* and *P2RX7* were up-regulated in DLBCL patient samples, whereas *P2RX1* was down-regulated in DLBCL patient samples (Fig. 1A). Then the GEO datasets GSE12195, GSE12453, GSE25639, GSE32018 were used to validate the expression level of the *P2RX7* [21–24]. Compared to normal tissues, *P2RX7* was significantly up-regulated in DLBCL patient samples (Fig. 1B). In addition, compared to samples from DLBCL patient without relapse, Fig. 1C indicated that the DNA copy numbers of P2X7 had a non-significant up-regulated trend in DLBCL samples from primary site, and significantly up-regulated in DLBCL samples from relapsing site in dataset GSE65720 [25]. Moreover, in datasets GSE57611, GSE56315, GSE74266, GSE32918 [26–29], the expression level of *P2RX7* had no significant difference between ABC subtype and GCB subtype in DLBCL patient samples (Fig. S1). These results mainly indicated that P2X7 was highly expressed in DLBCL patients.

To further explore the expression and function of P2X7 in DLBCL cells. Firstly, the GEO datasets GSE94669 and GSE27255 were used to evaluate the expression level of the

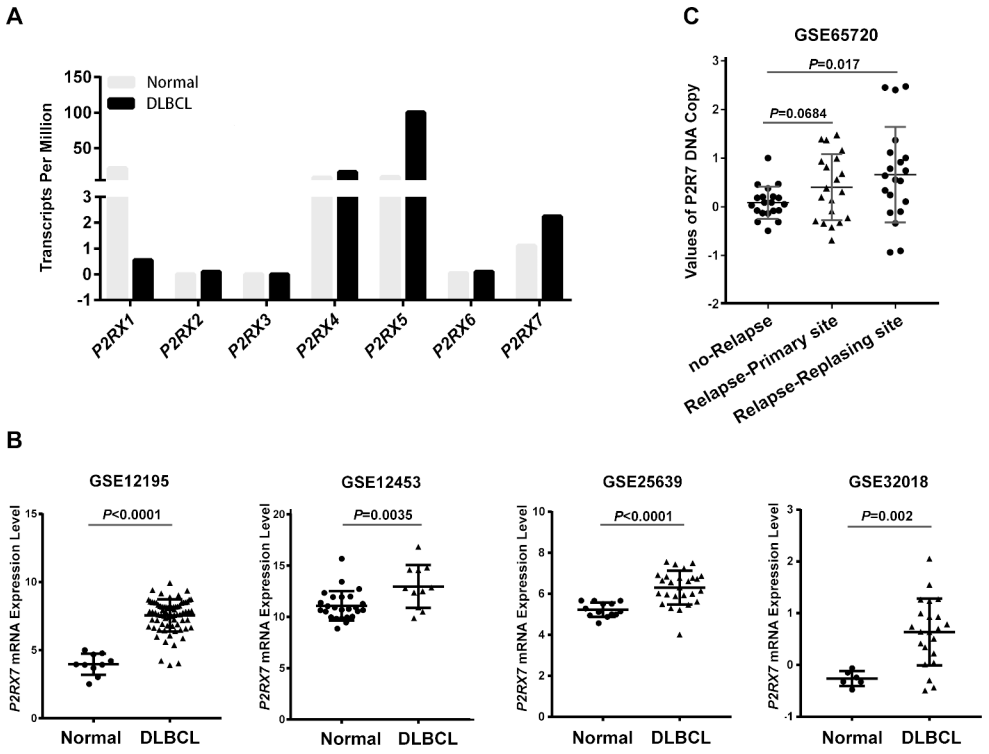

Fig. 1 Expression of the P2X7 receptor in DLBCL patients. The expression level of P2 *P2RX7* in DLBCL patients was analyzed with the GEPIA website tool and the GEO database. (**A**) The gene expression of P2X receptor family members between normal tissue (n = 337) and DLBCL samples (n = 47) from GEPIA. (**B**) The gene expression of *P2RX7* between normal tissue and DLBCL samples in datasets GSE12195 (normal n = 10, DLBCL n = 73), GSE12453 (normal n = 25, DLBCL n = 11), GSE25639 (normal n = 13, DLBCL n = 26), GSE32018 (normal n = 6, DLBCL n = 22) from GEO database. (**C**) The DNA copy number of P2X7 in DLBCL samples without relapse (n = 20), the primary site sample of relapsed DLBCL patient (n = 20) and the relapsing site sample of relapsed DLBCL patient (n = 20) in dataset GSE65720 from GEO database. Data were analyzed by unpaired Student's t-test. Each dot represents an individual normal or DLBCL patient sample

P2RX7 in DLBCL cell lines [30, 31]. As a result, *P2RX7* was widely expressed in both ABC and GCB subtype DLBCL cell lines samples, and only GCB-DLBCL cell lines Farage, RCK8 and WSU NIH expressed higher level of *P2RX7* (Fig. 2A and 2B). Then the expression level of *P2RX7* in ABC subtype DBCL cell line OCI-Ly3 and GCB subtype DBCL cell line SU-DHL-4 were validated by quantitative real time PCR. Previous work has demonstrated that K562 cells expressed low level of endogenous P2X7, so K562 cells was loaded as negative control [32]. Compared to K562 cells, OCI-Ly3 and SU-DHL-4 cells expressed abundant P2X7 receptors (Fig. 2C). We then assessed the Ca^{2+} influx function of P2X7 by Fura-2 fluorescence assay. The OCI-Ly3 and SU-DHL-4 were stimulated with Bz-ATP, a P2X7 agonist. Upon stimulation, the intracellular free Ca^{2+} concentration of OCI-Ly3 and SU-DHL-4 cells were both up-regulated, but pretreatment with A740003 completely impaired Bz-ATP-induced calcium fluxes (Fig. 2D). These findings suggested that P2X7 was widely expressed in various DLBCL cell lines and mediated Ca^{2+} influx upon activation.

P2X7 mediates DLBCL cells proliferation

To study the effect of P2X7 receptors on DLBCL cells proliferation, MTS assay was performed. Bz-ATP significantly promoted OCI-Ly3 and SU-DHL-4 cells proliferation (Fig. S2A, S2B and Fig. 3A), while P2X7 antagonist A740003 significantly inhibited OCI-Ly3 and SU-DHL-4 cells proliferation (Fig. S2C, S2D and Fig. 3B). To further validate the effect of P2X7 receptors on DLBCL cells proliferation, an EdU incorporation assay was performed. Administration of Bz-ATP in OCI-Ly3 and SU-DHL-4 resulted in an increase of proliferation as evidenced by more EdU incorporation, while A740003 resulted in a decrease of proliferation as evidenced by less EdU incorporation (Fig. 3C and 3D). These results were quantified and shown in Fig. 3E and 3F. Moreover, the effect of Bz-ATP on proliferation of OCI-Ly3 cells and SU-DHL-4 cells was attenuated by specific P2X7 blocker A740003 (Fig. S2E, S2F). Collectively, our data demonstrated that targeted-inhibition of P2X7 signaling can effectively suppress the proliferation of DLBCL cell.

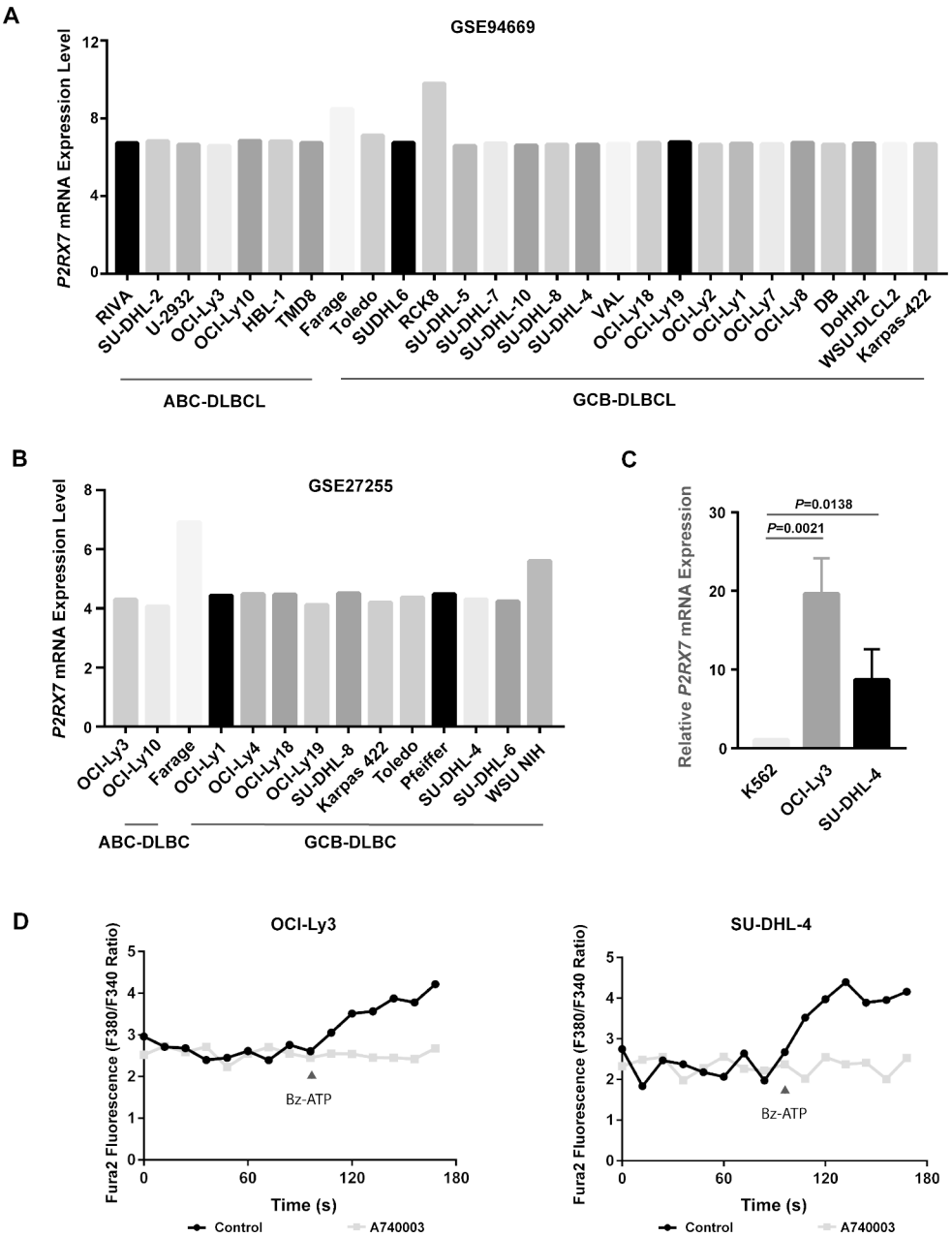

Fig. 2 Expression and Ca^{2+} influx function of the P2X7 receptor in DLBCL cell lines. (**A, B**) The expression level of *P2RX7* in ABC subtype and GCB subtype DLBCL cell lines were analyzed with datasets GSE94669 (**A**) and GSE27255 (**B**) from the GEO database. (**C**) The expression level of *P2RX7* in OCI-ly3 and SU-DHL-4 were validated by real time PCR. The RQ value of K562 was designated as 1.000. Results in panel C are presented as the mean ± SD of three independent experiments. Data were analyzed by unpaired Student's t-test. SD in K562 group appears absent, it is too small to be seen. (**D**) The Ca^{2+} influx function of P2X7 in OCI-ly3 and SU-DHL-4 was validated by measurement of intracellular free Ca^{2+} concentration upon activation. Cells were pre-treated with 20 μM A740003 or control lock's solution for 5 min respectively before administration with Bz-ATP. Triangle symbol indicates the addition of 50 μM Bz-ATP. The Fura-2 fluorescence at emission wavelength of 510 nm excited separately by wavelength of 340 or 380 nm were recorded, and the excitation ratio (340/380) was quantified at the indicated time point. Representative results from two independent experiments are shown

RNAseq of DLBCL cells with activated or inhibited P2X7 signaling

To gain further insights into molecular mechanism of P2X7 signaling in DLBCL cells, the gene expression profiles were determined by RNAseq (GSE225174). Accordingly, SU-DHL-4 cells were treated with PBS, Bz-ATP or A740003 for 48 h, then RNA was isolated, mRNA sequencing and counts were performed as indicated in methods section. DEGs were filtrated with these two criteria: FDR < 0.05 and FC > 2. Compared to PBS control, 44 genes were up-regulated and 14 genes were down-regulated in Bz-ATP group (Fig. S3A), while 55 genes were up-regulated and 17 genes were down-regulated in A740003 group (Fig. S3B). The up-regulated or down-regulated DEGs of Bz-ATP versus control and A740003 versus control were shown in a Venn diagram (Fig. 4A and 4B). Then total 140 DEGs were rearranged into 12 clusters based on their expression patterns in three samples by K-mean clustering method. Four clusters include: Cluster I (Bz-ATP down-regulated while both Control and A740003 up-regulated), Cluster II (Bz-ATP up-regulated while both Control and A740003 down-regulated), Cluster III (A740003 up-regulated while both Control and Bz-ATP down-regulated) and Cluster IV (A740003 down-regulated while both Control and Bz-ATP up-regulated) were highlighted, and typical genes were shown (Fig. 4C).

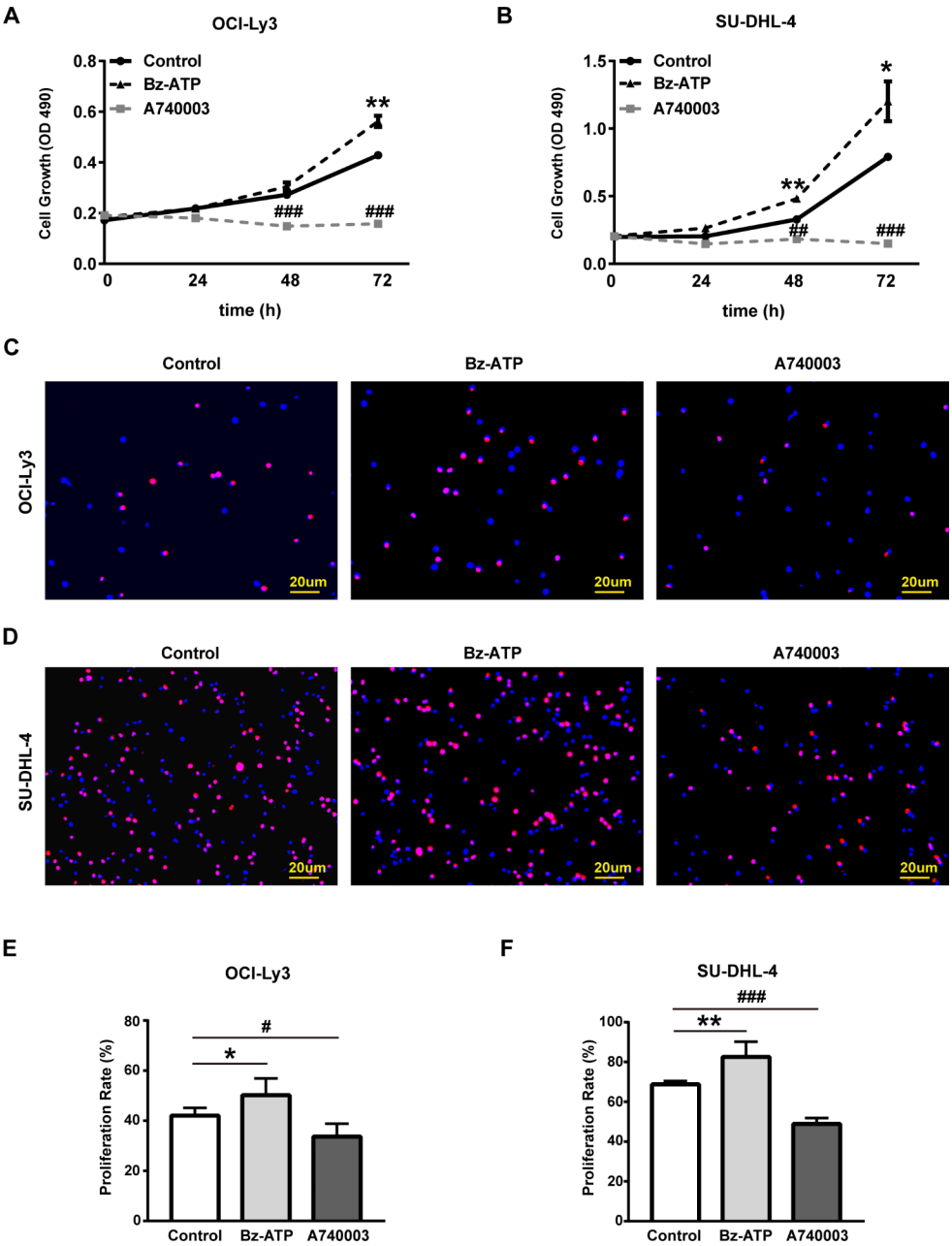

Fig. 3 P2X7 receptor signaling controls DLBCL cells proliferation. Cell proliferation (MTS) assays and EdU incorporation assays of OCI-Ly3 and SU-DHL-4 cells treated with P2X7 agonist Bz-ATP or P2X7 antagonist A740003. (**A, B**) OCI-Ly3 and SU-DHL-4 cells were treated with PBS, 50 μM BZ-ATP or 50 μM A740003 for 72 h. The proliferation of OCI-Ly3 (**A**) and SU-DHL-4 (**B**) cells were measured at the indicated time points by MTS assay. Results in panel A and panel B are presented as the mean ± SD of three independent experiments. Data were analyzed by unpaired Student's t-test. Partial SDs in panel A and panel B appear absent, they are too small to be seen. (**C-F**) OCI-Ly3 and SU-DHL-4 cells were treated with PBS, 50 μM Bz-ATP or 50 μM A740003 for 48 h. Then the cells were incubated with 50 μM EdU for 2 h which was detected using a click reaction kit by fluorescence microscope. The representative image of proliferating OCI-Ly3 (**C**) and SU-DHL-4 (**D**) cells from three independent experiments were shown (DAPI-blue$^+$, EdU-red$^+$). Scale bars: 20 μm. Percentage of proliferating OCI-Ly3 (**E**) and SU-DHL-4 (**F**) cells were quantified with 5 random section by Image J. Results in panel E and panel F are presented as the mean ± SD. Data were analyzed by unpaired Student's t-test. Bz-ATP vs. Control: *$p < 0.05$, **$p < 0.01$, ***$p < 0.001$. A740003 vs. Control: #$p < 0.05$, ##$p < 0.01$, ###$p < 0.001$

Moreover, three genes (*TLCD1*, *ABCA7*, *ICAM5*) in cluster II and three genes (*RN7SL1*, *SLX1B*, *DHRS2*) in cluster III were validated by qRT-PCR (Fig. 4D). Furthermore, KEGG results showed that *Galactose metabolism*, *Starch and sucrose metabolism*, *Amino sugar and nucleotide sugar metabolism* were enriched in Bz-ATP group (genes in cluster I and cluster II) and shown in Fig. 4E. *Fatty acid metabolism*, *Pyrimidine metabolism*, *Purine metabolism* were enriched in A740003 group (genes in cluster III and cluster IV) and shown in Fig. 4F. These results suggest that P2X7 signaling may control DLBCL cells proliferation by mediating cellular metabolism pathway.

CPS1 was involved in DLBCL cells proliferation regulated by P2X7 signaling

To identify the key molecular mediated by P2X7 signaling in DLBCL cells, we firstly listed genes associated with purine metabolism and pyrimidine metabolism in our RNAseq data. Importantly, only *CPS1* was up-regulated in Bz-ATP group while down-regulated in A740003 group (Fig. 5A and 5B). In addition, the relative expression of *P2RX7* and *CPS1* from the DLBCL patient dataset GSE12195 was assessed in Fig. 5C [21]. Moreover, significantly decrease of *CPS1* was observed in DLBCL cells upon A740003 administration (Fig. 5D). CPS1 plays a crucial role in removing excessive

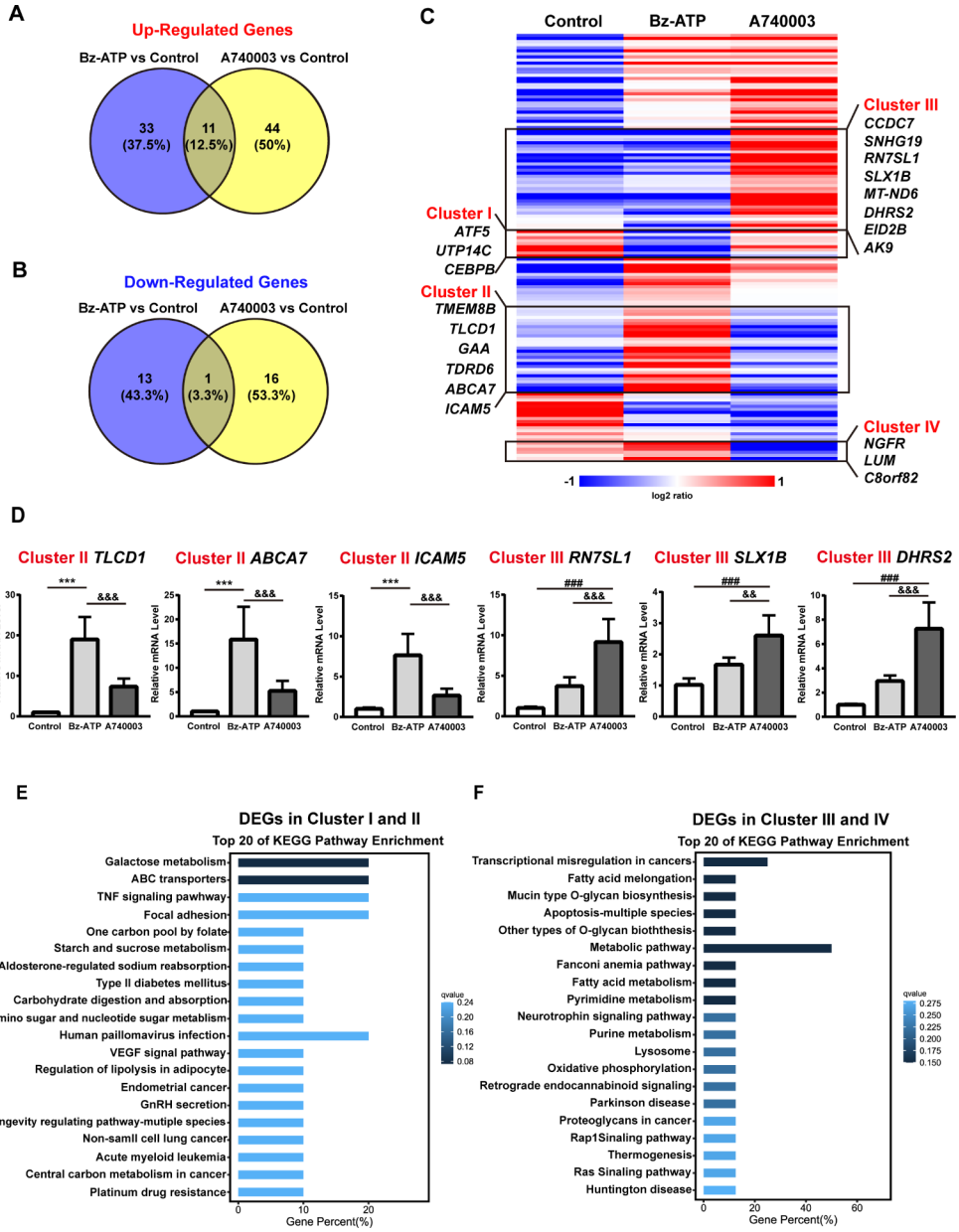

Fig. 4 Gene expression profiles of DLBCL cells with P2X7 activation or P2X7 inhibition. SU-DHL-4 cells were treated with PBS, 50 μM BZ-ATP or 50 μM A740003 for 48 h. Then cells were collected and RNAseq was performed. (**A, B**) The Venn diagram illustrates number of overlapped up-regulated DEGs (**A**) and down-regulated DEGs (**B**) in DLBCL cells. (**C**) K-mean clustering of 140 DEGs were performed. Typical DEGs in Cluster I (Bz-ATP down-regulated while both Control and A740003 up-regulated), Cluster II (Bz-ATP up-regulated while both Control and A740003 down-regulated), Cluster III (A740003 up-regulated while both Control and Bz-ATP down-regulated) and Cluster IV (A740003 down-regulated while both Control and Bz-ATP up-regulated) were shown. (**D**) The genes in Cluster II and Cluster III were validated by real time PCR. The RQ value of Control group treated with PBS was designated as 1.000. Results in panel D are presented as the mean ± SD of three independent experiments. Data were analyzed by unpaired Student's t-test. Partial SDs in control group appear absent, they are too small to be seen. (**E, F**) KEGG pathway analysis were performed with DEGs from Cluster I and II (**E**), Cluster III and IV (**F**), the abscissa is the percentage of the number of genes in the KEGG pathway analysis to the total number of differentially expressed genes, the ordinate is the name of KEGG pathway, color indicates the q value (enriched adjusted P-value, lower value indicates higher significance). The KEGG pathways with top 20 minimum q value were shown. Bz-ATP vs. Control: $*p < 0.05$, $**p < 0.01$, $***p < 0.001$. A740003 vs. Control: $\#p < 0.05$, $\#\#p < 0.01$, $\#\#\#p < 0.001$. Bz-ATP vs. A740003: $\&p < 0.05$, $\&\&p < 0.01$, $\&\&\&p < 0.001$

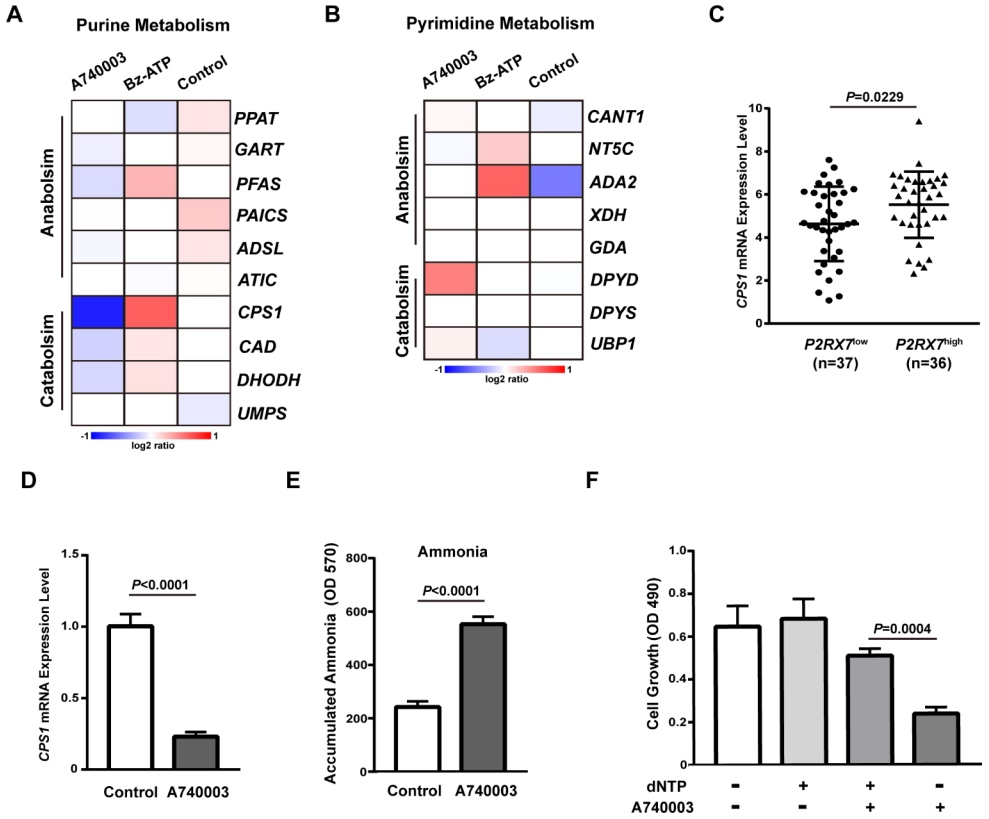

Fig. 5 P2X7 receptors mediating proliferation of DLBCL cells by CPS1 (**A, B**) The expression level of genes associated with purine metabolism (**A**) and pyrimidine metabolism (**B**) from RNAseq data. (**C**) The relative expression of *P2RX7* and *CPS1* was analyzed with the GSE12195 (n = 73) dataset from GEO database. Data were analyzed by unpaired Student's t-test. Each dot represents an individual DLBCL patient sample. (**D**) The expression level of *CPS1* in SU-DHL-4 treated with PBS or 50 μm A740003 were validated by real time PCR. The RQ value of Control group treated with PBS was designated as 1.000. (**E**) Ammonia was statistically significantly accumulated in the media of SU-DHL-4 cells treated with A740003 compared to control. (**F**) MTS assay of SU-DHL-4 cells treated with A740003 in combination with or without 100 μM dNTP. Results in panel D, panel E and panel F are presented as the mean ± SD of three independent experiments. Data were analyzed by unpaired Student's t-test

ammonia by converting ammonium into carbamoyl phosphate, which is a de novo resource of arginine and potential substrate of pyrimidine synthesis [33, 34]. As expected, administration of A740003 significantly increased levels of ammonia in the media (Fig. 5E). Furthermore, supplementation of deoxynucleotide (dNTP) significantly rescued cell growth in cells with A740003 (Fig. 5F). Taken together, the results show that CPS1 was involved in P2X7 signaling mediated proliferation of DLBCL cells.

Discussion

DLBCL is a type of aggressive hematopoietic malignancy. Standard R-CHOP therapy only achieves disease-free survival in nearly 60% of DLBCL patients [35]. However, approximately 33% of DLBCL patients are refractory or relapses to R-CHOP therapy, and the prognosis is generally poor [36]. Although transplant-eligible rrDLBCL patients are treated with intensive salvage regimens followed by high-dose chemotherapy and autologous stem cell transplantation (ASCT), only few patients are cured [37]. Until now, various novel antibodies, specific small-molecule inhibitors, antibody drug conjugates (ADCs), as well as CAR T-cells have been approved for the treatment of DLBCL patients [38, 39]. But knowledge about why some patients respond to specific therapies while others are resistant, remains very limited. Hence, the molecular mechanism of how the novel targets promote DLBCL progression need to be fully elucidated. Most recently, purinergic signaling, typically extracellular ATP activated purinergic signaling recognized by P2X7 receptor, has been suggested as a prospective therapeutic target in hematopoietic malignancy [12]. In our previous study, we observed that P2X7 is preferentially expressed in mature hematopoietic cells than HSPCs, but overexpression of P2X7 in HPSCs could not transform normal HSPCs into leukemia cells [13]. Interestingly, our further study showed that P2X7 accelerates the progression of MLL-AF9 (mixed lineage leukemia-AF9 fusion gene) induced AML by promoting proliferation and increasing LSC through the

upregulation of Pbx3 [14]. However, little is known about the effects of P2X7 on DLBCL cells. In the present study, P2X7 was demonstrated aberrantly up-regulated in patients with DLBCL, particularly expressed in relapsed site of DLBCL patient samples. Furthermore, Bz-ATP promoted the proliferation of DLBCL cells, while inhibited proliferation was detected when administrated with P2X7 antagonist A740003. Moreover, CPS1 mediated purine metabolism pathway was involved in this process. Our results not only elucidate the significance of the P2X7 in the progression of DLBCL but also provide new insights for the research and clinical therapy of hematopoietic malignancy.

Based on gene expression signature, DLBCLs are classified into activated B-cell-like (ABC-DLBCL) and germinal center B-cell-like (GCB-DLBCL) subtypes [40]. ABC-DLBCL displays chronically active BCR signaling, resulting in constitutive NF-κB activity [3]. On the other hand, a subset of GCB-DLBCLs rely on the activation of PI3K signaling induced by tonic B-cell receptor (BCR) signaling [41]. Although ABC-DLBCL and GCB-DLBCL have different mutation profiles and response differently to standard immune-chemotherapy [5]. In this study, we found no significant difference between ABC-DLBCL patients and GCB-DLBCL patients in *P2RX7* expression. Moreover, the proliferation of ABC-DLBCL cell line OCI-Ly3 or GCB-DLBCL cell line SU-DHL-4, were both effectively modulated by P2X7 signaling. Hence, our result confirmed that purinergic signaling mediated by P2X7 receptor exerted similar effects on proliferation of both ABC-DLBCL and GCB-DLBCL tumor cells.

P2RX7 is highly polymorphic and contains several splice variants, which includes: *P2RX7A* (the wide type *P2RX7*, NM_002562.6), *P2RX7B* (AY847298), *P2RX7C* (AY847299), *P2RX7D* (AY847300.1), *P2RX7E* (AY847301.1), *P2RX7F* (AY847302.1), *P2RX7G* (AY847303.1), *P2RX7H* (AY847304.1), *P2RX7L* (MK465687.1), *P2RX7N* (MK465688.1), *P2RX7O* (MK465689.1), *P2RX7P* (MK465690.1), *P2RX7Q* (MK465691.1). Most Importantly, recent studies have shown that P2X7-mediated cell proliferation is largely induced by the P2X7B isoform in AML, osteosarcomas, glioblastoma, etc. [42–45]. Our results have demonstrated that target-inhibit P2X7 receptor could attenuate the proliferation of DLBCL cells. However, which isoform of *P2RX7* plays critical role in this process and the involved molecular mechanisms still need to be further discussed and studied in the future.

The interaction between extracellular ATP and P2X7 receptor affects tumor progression by controlling the activity of downstream kinase-dependent signaling pathways and transcription factors [46]. Although early studies suggested that exposure to high levels of ATP will activate PI3K/AKT axis and AMPK-PRAS40-mTOR pathway, which lead to cell death by disrupting the balance between cell growth and autophagy in colon cancer [47]. Recent studies have reported that abundantly extracellular ATP in the tumor microenvironment plays a critical role in promoting tumor cells proliferation, survival and drug resistance depending on chronic P2X7-activated calcium influx in neuroblastoma, non-melanoma skin cancer, prostate cancer and thyroid papillary cancer [6]. The sustained calcium influx sequentially activated ERK/PI3K/MEK pathway and induced the release of cytokines, inflammatory factors or microparticles, and finally promote the proliferation and metastasis of tumor cells [12]. Interestingly, based on the bioinformatics analysis of RNAseq data, the KEGG result shows that P2X7 regulated proliferation of DLBCL may mainly through metabolic pathways. DEGs in Bz-ATP group enriched in galactose metabolism, starch and sucrose metabolism, amino sugar and nucleotide sugar metabolism. DEGs in P2X7-inhibited DLBCL cells enriched in fatty acid metabolism, pyrimidine metabolism, purine metabolism. When we focus on the genes associated with pyrimidine and purine metabolism, *CSP1* was screened out, for its upregulation in Bz-ATP group while downregulation in A740003 group. These results suggest that CPS1 may be largely involved in the proliferation of DLBCL cells induced by P2X7 signaling.

CPS1 is a multidomain mitochondrial enzyme protein, catalyzing the first committed step of the urea cycle for ammonia detoxification and disposal [33, 48]. CPS1 is involved in the purine and pyrimidine metabolism pathways, which remove excessive ammonia by converting ammonium into carbamoyl phosphate [34]. Knockdown of CPS1 induced accumulation of ammonia, a decrease of metabolites in nucleic acid synthesis pathways [49]. We firstly demonstrated that the expression of *CPS1* is positively correlated with *P2RX7* in the samples of DLBCL patients. Administration of P2X7 antagonist A740003 significantly down-regulated the expression of *CPS1*, which subsequently induced accumulation of ammonia. Moreover, exogenous supplementation of dNTP successfully rescued the A740003 suppressed proliferation of DLBCL cells. Therefore, these results suggested that P2X7 may promote/inhibit the proliferation of DLBCL cells through CPS1. Further work is needed to elucidate the detailed interactions between P2X7 and CPS1.

In summary, the expression level of P2X7 is aberrantly up-regulated in patients with DLBCL. P2X7 signaling modulate the proliferation of OCI-Ly3 and SU-DHL-4 cells. Most importantly, CPS1 associated purine and pyrimidine metabolic pathway is involved in this process. This work reveals the role of P2X7 in the proliferation of DLBCL cells and implies that P2X7 may serve as a potential molecular target for the treatment of rrDLBCL.

Supplementary Information The online version contains supplementary material available at https://doi.org/10.1007/s11302-023-09947-w.

Author contributions Xiao Yang acquired funding, designed and performed experiments, analyzed and interpreted data and wrote the manuscript. Yuanyuan Ji designed experiments, interpreted data. Lin Mei, Wenwen Jing and Xin Yang performed experiments, analyzed and interpreted data. Qianwei Liu analyzed and interpreted data. All authors contributed to the article and approved the submitted version.

Funding This work was supported by grant 2020JQ-546 from the Natural Science Basic Research Program of Shaanxi; grant 81802862 from the National Natural Science Foundation of China (NSFC); the Personnel Training Specialized Research Foundation RC(XM)202002 from the Second Affiliated Hospital of Xi'an Jiaotong University.

Data availability The data that had been used for the findings of this research project are available from the corresponding author upon reasonable request.

Declarations

Competing interests The authors declare no other competing interests.

Conflict of interest The authors declare that there is no conflict of interest.

Ethical approval Not applicable.

References

1. Chapuy B, Stewart C, Dunford AJ, Kim J, Kamburov A, Redd RA et al (2018) Molecular subtypes of diffuse large B cell lymphoma are associated with distinct pathogenic mechanisms and outcomes. Nat Med 24:679–690. https://doi.org/10.1038/s41591-018-0016-8
2. Pasqualucci L, Dalla-Favera R (2014) SnapShot: diffuse large B cell lymphoma. Cancer Cell 25:132–132. e131. https://doi.org/10.1016/j.ccr.2013.12.012
3. Davis RE, Ngo VN, Lenz G, Tolar P, Young RM, Romesser PB et al (2010) Chronic active B-cell-receptor signalling in diffuse large B-cell lymphoma. Nature 463:88–92. https://doi.org/10.1038/nature08638
4. Lenz G, Davis RE, Ngo VN, Lam L, George TC, Wright GW et al (2008) Oncogenic CARD11 mutations in human diffuse large B cell lymphoma. Science 319:1676–1679. https://doi.org/10.1126/science.1153629
5. Kaur J, Dora S (2023) Purinergic signaling: diverse effects and therapeutic potential in cancer. Front Oncol 13:1058371. https://doi.org/10.3389/fonc.2023.1058371
6. Di Virgilio F, Sarti AC, Falzoni S, De Marchi E, Adinolfi E (2018) Extracellular ATP and P2 purinergic signalling in the tumour microenvironment. Nat Rev Cancer 18:601–618. https://doi.org/10.1038/s41568-018-0037-0
7. Burnstock G, Di Virgilio F (2013) Purinergic signalling and cancer. Purinergic Signal 9:491–540. https://doi.org/10.1007/s11302-013-9372-5
8. Mai Y, Guo Z, Yin W, Zhong N, Dicpinigaitis PV, Chen R (2021) P2X receptors: potential therapeutic targets for symptoms Associated with Lung Cancer - A Mini Review. Front Oncol 11:691956. https://doi.org/10.3389/fonc.2021.691956
9. Nagel D, Vincendeau M, Eitelhuber AC, Krappmann D (2014) Mechanisms and consequences of constitutive NF-kappaB activation in B-cell lymphoid malignancies. Oncogene 33:5655–5665. https://doi.org/10.1038/onc.2013.565
10. Jelassi B, Chantome A, Alcaraz-Perez F, Baroja-Mazo A, Cayuela ML, Pelegrin P et al (2011) P2X(7) receptor activation enhances SK3 channels- and cystein cathepsin-dependent cancer cells invasiveness. Oncogene 30:2108–2122. https://doi.org/10.1038/onc.2010.593
11. Burnstock G (2016) P2X ion channel receptors and inflammation. Purinergic Signal 12:59–67. https://doi.org/10.1007/s11302-015-9493-0
12. Burnstock G, Knight GE (2018) The potential of P2X7 receptors as a therapeutic target, including inflammation and tumour progression. Purinergic Signal 14:1–18. https://doi.org/10.1007/s11302-017-9593-0
13. Feng W, Yang F, Wang R, Yang X, Wang L, Chen C et al (2016) High level P2X7-Mediated signaling impairs function of hematopoietic Stem/Progenitor cells. Stem Cell Rev Rep 12:305–314. https://doi.org/10.1007/s12015-016-9651-y
14. Feng W, Yang X, Wang L, Wang R, Yang F, Wang H et al (2021) P2X7 promotes the progression of MLL-AF9 induced acute myeloid leukemia by upregulation of Pbx3. Haematologica 106:1278–1289. https://doi.org/10.3324/haematol.2019.243360
15. Morgan R, Pandha HS (2020) PBX3 in Cancer. Cancers (Basel) 12. https://doi.org/10.3390/cancers12020431
16. Adinolfi E, Melchiorri L, Falzoni S, Chiozzi P, Morelli A, Tieghi A et al (2002) P2X7 receptor expression in evolutive and indolent forms of chronic B lymphocytic leukemia. Blood 99:706–708. https://doi.org/10.1182/blood.v99.2.706
17. He X, Wan J, Yang X, Zhang X, Huang D, Li X et al (2021) Bone marrow niche ATP levels determine leukemia-initiating cell activity via P2X7 in leukemic models. J Clin Invest 131. https://doi.org/10.1172/JCI140242
18. Illes P, Muller CE, Jacobson KA, Grutter T, Nicke A, Fountain SJ et al (2021) Update of P2X receptor properties and their pharmacology: IUPHAR Review 30. Br J Pharmacol 178:489–514. https://doi.org/10.1111/bph.15299
19. Tang Z, Li C, Kang B, Gao G, Li C, Zhang Z (2017) GEPIA: a web server for cancer and normal gene expression profiling and interactive analyses. Nucleic Acids Res 45:W98–W102. https://doi.org/10.1093/nar/gkx247
20. Wagner GP, Kin K, Lynch VJ (2012) Measurement of mRNA abundance using RNA-seq data: RPKM measure is inconsistent among samples. Theory Biosci 131:281–285. https://doi.org/10.1007/s12064-012-0162-3
21. Compagno M, Lim WK, Grunn A, Nandula SV, Brahmachary M, Shen Q et al (2009) Mutations of multiple genes cause deregulation of NF-kappaB in diffuse large B-cell lymphoma. Nature 459:717–721. https://doi.org/10.1038/nature07968
22. Brune V, Tiacci E, Pfeil I, Doring C, Eckerle S, van Noesel CJ et al (2008) Origin and pathogenesis of nodular lymphocyte-predominant Hodgkin lymphoma as revealed by global gene expression analysis. J Exp Med 205:2251–2268. https://doi.org/10.1084/jem.20080809
23. Vicente-Duenas C, Fontan L, Gonzalez-Herrero I, Romero-Camarero I, Segura V, Aznar MA et al (2012) Expression of MALT1 oncogene in hematopoietic stem/progenitor cells recapitulates the pathogenesis of human lymphoma in mice. Proc Natl Acad Sci U S A 109:10534–10539. https://doi.org/10.1073/pnas.1204127109
24. Gomez-Abad C, Pisonero H, Blanco-Aparicio C, Roncador G, Gonzalez-Menchen A, Martinez-Climent JA et al (2011) PIM2 inhibition as a rational therapeutic approach in B-cell lymphoma. Blood 118:5517–5527. https://doi.org/10.1182/blood-2011-03-344374

25. Juskevicius D, Lorber T, Gsponer J, Perrina V, Ruiz C, Stenner-Liewen F et al (2016) Distinct genetic evolution patterns of relapsing diffuse large B-cell lymphoma revealed by genome-wide copy number aberration and targeted sequencing analysis. Leukemia 30:2385–2395. https://doi.org/10.1038/leu.2016.135
26. Scholtysik R, Kreuz M, Hummel M, Rosolowski M, Szczepanowski M, Klapper W et al (2015) Characterization of genomic imbalances in diffuse large B-cell lymphoma by detailed SNP-chip analysis. Int J Cancer 136:1033–1042. https://doi.org/10.1002/ijc.29072
27. Dybkaer K, Bogsted M, Falgreen S, Bodker JS, Kjeldsen MK, Schmitz A et al (2015) Diffuse large B-cell lymphoma classification system that associates normal B-cell subset phenotypes with prognosis. J Clin Oncol 33:1379–1388. https://doi.org/10.1200/JCO.2014.57.7080
28. Marques SC, Ranjbar B, Laursen MB, Falgreen S, Bilgrau AE, Bodker JS et al (2016) High miR-34a expression improves response to doxorubicin in diffuse large B-cell lymphoma. Exp Hematol 44:238–246e232. https://doi.org/10.1016/j.exphem.2015.12.007
29. Barrans SL, Crouch S, Care MA, Worrillow L, Smith A, Patmore R et al (2012) Whole genome expression profiling based on paraffin embedded tissue can be used to classify diffuse large B-cell lymphoma and predict clinical outcome. Br J Haematol 159:441–453. https://doi.org/10.1111/bjh.12045
30. Tarantelli C, Gaudio E, Arribas AJ, Kwee I, Hillmann P, Rinaldi A et al (2018) PQR309 is a Novel Dual PI3K/mTOR inhibitor with Preclinical Antitumor Activity in Lymphomas as a single Agent and in combination therapy. Clin Cancer Res 24:120–129. https://doi.org/10.1158/1078-0432.CCR-17-1041
31. Petrich AM, Leshchenko V, Kuo PY, Xia B, Thirukonda VK, Ulahannan N et al (2012) Akt inhibitors MK-2206 and nelfinavir overcome mTOR inhibitor resistance in diffuse large B-cell lymphoma. Clin Cancer Res 18:2534–2544. https://doi.org/10.1158/1078-0432.CCR-11-1407
32. Chong JH, Zheng GG, Ma YY, Zhang HY, Nie K, Lin YM et al (2010) The hyposensitive N187D P2X7 mutant promotes malignant progression in nude mice. J Biol Chem 285:36179–36187. https://doi.org/10.1074/jbc.M110.128488
33. Summar ML, Dasouki MJ, Schofield PJ, Krishnamani MR, Vnencak-Jones C, Tuchman M et al (1995) Physical and linkage mapping of human carbamyl phosphate synthetase I (CPS1) and reassignment from 2p to 2q35. Cytogenet Cell Genet 71:266–267. https://doi.org/10.1159/000134124
34. Morris SM Jr (2002) Regulation of enzymes of the urea cycle and arginine metabolism. Annu Rev Nutr 22:87–105. https://doi.org/10.1146/annurev.nutr.22.110801.140547
35. Coiffier B, Sarkozy C (2016) Diffuse large B-cell lymphoma: R-CHOP failure-what to do? Hematol Am Soc Hematol Educ Program 2016:366–378. https://doi.org/10.1182/asheducation-2016.1.366
36. Sehn LH, Berry B, Chhanabhai M, Fitzgerald C, Gill K, Hoskins P et al (2007) The revised International Prognostic Index (R-IPI) is a better predictor of outcome than the standard IPI for patients with diffuse large B-cell lymphoma treated with R-CHOP. Blood 109:1857–1861. https://doi.org/10.1182/blood-2006-08-038257
37. Gisselbrecht C, Glass B, Mounier N, Singh Gill D, Linch DC, Trneny M et al (2010) Salvage regimens with autologous transplantation for relapsed large B-cell lymphoma in the rituximab era. J Clin Oncol 28:4184–4190. https://doi.org/10.1200/JCO.2010.28.1618
38. Chen YJ, Abila B, Mostafa Kamel Y (2023) CAR-T: what is next? Cancers. 15. https://doi.org/10.3390/cancers15030663
39. Del Toro-Mijares R, Oluwole O, Jayani RV, Kassim AA, Savani BN, Dholaria B (2023) Relapsed or refractory large B-cell lymphoma after chimeric antigen receptor T-cell therapy: current challenges and therapeutic options. Br J Haematol. https://doi.org/10.1111/bjh.18656
40. Alizadeh AA, Eisen MB, Davis RE, Ma C, Lossos IS, Rosenwald A et al (2000) Distinct types of diffuse large B-cell lymphoma identified by gene expression profiling. Nature 403:503–511. https://doi.org/10.1038/35000501
41. Chen L, Monti S, Juszczynski P, Ouyang J, Chapuy B, Neuberg D et al (2013) SYK inhibition modulates distinct PI3K/AKT-dependent survival pathways and cholesterol biosynthesis in diffuse large B cell lymphomas. Cancer Cell 23:826–838. https://doi.org/10.1016/j.ccr.2013.05.002
42. Adinolfi E, Cirillo M, Woltersdorf R, Falzoni S, Chiozzi P, Pellegatti P et al (2010) Trophic activity of a naturally occurring truncated isoform of the P2X7 receptor. FASEB J 24:3393–3404. https://doi.org/10.1096/fj.09-153601
43. Giuliani AL, Colognesi D, Ricco T, Roncato C, Capece M, Amoroso F et al (2014) Trophic activity of human P2X7 receptor isoforms a and B in osteosarcoma. PLoS ONE 9:e107224. https://doi.org/10.1371/journal.pone.0107224
44. Pegoraro A, Orioli E, De Marchi E, Salvestrini V, Milani A, Di Virgilio F et al (2020) Differential sensitivity of acute myeloid leukemia cells to daunorubicin depends on P2X7A versus P2X7B receptor expression. Cell Death Dis 11:876. https://doi.org/10.1038/s41419-020-03058-9
45. Zanoni M, Sarti AC, Zamagni A, Cortesi M, Pignatta S, Arienti C et al (2022) Irradiation causes senescence, ATP release, and P2X7 receptor isoform switch in glioblastoma. Cell Death Dis 13:80. https://doi.org/10.1038/s41419-022-04526-0
46. He X, Zhang Y, Xu Y, Xie L, Yu Z, Zheng J (2021) Function of the P2X7 receptor in hematopoiesis and leukemogenesis. Exp Hematol 104:40–47. https://doi.org/10.1016/j.exphem.2021.10.001
47. Bian S, Sun X, Bai A, Zhang C, Li L, Enjyoji K et al (2013) P2X7 integrates PI3K/AKT and AMPK-PRAS40-mTOR signaling pathways to mediate Tumor Cell Death. PLoS ONE 8:e60184. https://doi.org/10.1371/journal.pone.0060184
48. Butler SL, Dong H, Cardona D, Jia M, Liu C (2008) The antigen for Hep Par 1 antibody is the urea cycle enzyme carbamoyl phosphate synthetase 1. Lab Invest 88:78–88. https://doi.org/10.1038/labinvest.3700699
49. elikta M, Tanaka I, Tripathi SC, Fahrmann JF, Aguilar-Bonavides C, Villalobos P et al (2017) Role of CPS1 in cell growth, metabolism, and prognosis in LKB1-Inactivated lung adenocarcinoma. J Natl Cancer Inst 109:1. https://doi.org/10.1093/jnci/djw231